

## Design and Evaluation of a Multi-Mode Robotic Arm Orthosis using Musculoskeletal Simulation

Erkan ÖDEMİŞ\*<sup>1</sup>, Cabbar Veysel BAYSAL<sup>1</sup>

<sup>1</sup>Çukurova Üniversitesi, Mühendislik Fakültesi, Biyomedikal Mühendisliği Bölümü, Adana

Geliş tarihi: 02.05.2018

Kabul tarihi: 15.10.2018

### Abstract

Robotic upper extremity orthoses have been used in rehabilitation for therapy of neuromuscular disorders and successful implementations are demonstrated by numerous clinical results. Majority of researchers focused on orthotic devices enabling basic therapy mode operations. However, there is still need for new orthotic designs which facilitates therapy modes and assistance for daily life activities in coherence. In this work, design of a multi-mode two DoF robotic arm orthosis is introduced. The designed robotic orthosis is implemented in simulation and tested with a human arm musculoskeletal model, for compliant operation. It uses model based computed torque controller and is tested for multi-mode operation. The performance is evaluated for compliant operation of “Assistive” and “Resistive” rehabilitation modes. Performance tests yielded encouraging results for future developments.

**Keywords:** Robotic arm orthosis, Model-based controller, Musculoskeletal modelling, Simulation

### Çok-Düzenli Robotik Kol Ortezinin Kas-iskelet Modeli Kullanılarak Tasarımı ve Performans Değerlendirmesi

#### Öz

Robotik kol ortezleri, motor-kas becerilerini kaybetmiş hastaların tedavisinde kullanılan ve başarıları sayısız klinik çalışmayla kanıtlanmış cihazlardır. Bu alandaki araştırmaların çoğu temel terapi düzeni operasyonlarını sağlayan ortotik cihazlara odaklanmıştır. Bununla birlikte terapi düzenlerini ve günlük aktiviteler için desteği uyumlu gerçekleştirebilecek yeni ortotik cihaz tasarımlarına hala ihtiyaç vardır. Bu çalışmada çok düzenli, iki serbestlik derecesine sahip bir ortez tasarımı yapılmıştır. Tasarlanan ortez uyumlu çalışma becerisi açısından bir kas-iskelet modeli üzerinde benzetim ortamında denenmiştir. Ortez, model tabanlı hesaplamalı tork kontrolcü kullanılmaktadır ve çok düzenli çalışma için test edilmiştir. Ortezin performansı “Yardımcı” ve “Dirençli” rehabilitasyon düzenlerinin uyumlu çalışması açısından değerlendirilmiştir. Performans testleri ileride yapılacak geliştirmeler için cesaret verici sonuçlar vermektedir.

**Anahtar Kelimeler:** Robotik kol ortezi, Model-tabanlı kontrolcü, Kas-iskelet modeli, Benzetim

---

\*Corresponding author (Sorumlu yazar): Erkan ÖDEMİŞ, [eodemis@cu.edu.tr](mailto:eodemis@cu.edu.tr)

## **1. INTRODUCTION**

Many people lose their neuromuscular abilities due to accidents and illnesses which affect their daily life negatively. Physiotherapy and rehabilitation are widely used methods for treating patients with neuromuscular disabilities. In traditional manner, exercises are performed with therapists but there are some disadvantages such as not enough time being spent with each patient or performance reduction in exercises due overloading. On the other hand, performing exercises with robotic devices has appeared as a new approach to overcome disadvantages of traditional treatment methods mentioned above [1,2].

Robotic rehabilitation devices have many advantages such as eliminating constraints on therapy time, giving the opportunity of local treatment under suitable conditions, facilitating evaluation and understanding the changes in patient's condition. Robotic rehabilitation devices can be classified according to their applied segment such as lower limb, upper limb or whole body [3]. Robotic orthoses are assistant devices fixed to the body to increase the performance of the limbs with partial functional losses. Robotic arm orthosis for rehabilitation belong to the upper extremity class of the rehabilitation devices [4]. Patients can perform rehabilitation exercises with these devices in different modes such as assistive, resistive, and repetitive [4,5]. The devices with active assistance help patients with daily activities like reaching and grasping [5]. In assistive exercises, the device helps patients complete the intended movements by applying external force [6]. Resistive mode in contrast to assistive mode aims to make patient spend more effort by adding some disruptive effects to the patient's movement [6].

The robotic arm orthoses could also be categorized according to mechanical designs and control methods [3,5,7]. The mechanical designs are classified with respect to number of joints, actuators used for motion and power transmission methods [3,4]. Different types of actuators are used such as pneumatic actuators, hydraulic actuators and motors [7]. Power transmission can be either gear driven or cable driven systems [3,4].

Controllers used in robotic orthotic devices could be grouped as model based, hierarchy based and physical parameters based control systems [8].

Model based control strategies can be grouped into dynamic model based controllers and muscle model based controllers [7]. The dynamic model is derived through modeling the human body as rigid links joined together by joints [8]. This model tries to estimate the torque produced by inertia, gravitational, coriolis and centrifugal effects [9]. Unlike the dynamic model, muscle model estimates the muscle moment as a function of muscle activation level and joint kinematics [8]. In muscle model, the input is EMG signal and the output is the force estimation [10].

Hierarchy based control can be studied at three levels: Task level, high level and low level. [8]. Task level control involves the highest level controller which produces command signals according to tasks designed in controller structure. The next controller level is the high level controller. It is responsible for the control of the force and position of the human-orthosis interaction according to the command signals from the task level controller. The high level controller is generally impedance and admittance controllers [11–14]. Lowest in the hierarchy is the low level controller. It is generally force and position controllers [10,13]. Physical parameter based controllers can be classified under three groups such as position controller, torque/force controller and force interaction controller [8].

In this work, we propose, a multi-mode robotic arm orthosis which enables assistive and resistive modes in coherence, as well as providing an opportunity for easy transition between these modes. In our orthosis implementation, rehabilitation exercises and assistance for daily activities could be done with same device, in contrast to many other single mode orthotic devices [6,9,10]. The designed robotic arm orthosis uses model-based computed torque controller due to its simplicity and stability. The designed orthosis was tested with a human arm musculoskeletal model in order to evaluate the multi-mode performance in simulation. The design

approach using musculoskeletal simulation could be utilized as an evaluation criterion for future stages of hardware implementation. In the following sections, design and implementation stages with simulation results are presented.

## 2. MATERIALS AND METHODS

In this work, design of a multi-mode robotic arm orthosis, which enables assistive and resistive rehabilitation modes, was proposed. Rehabilitation modes and mode transitions have been tested with the musculoskeletal model that has been designed in the MSMS (Musculoskeletal Modelling Software) and Matlab/Simulink [15]. The software packages were used for simulating the design of the musculoskeletal model in combination. The orthosis mechanical design has been exported to Matlab/Simmechanics environment. Model based computed torque controller was used for the control of orthotic device meanwhile the activation signals for the musculoskeletal model were controlled by a separate proportional–integral–derivative (PID) controller. The performance evaluation of the orthosis is done with respect to simulation results. The simulation yielded encouraging results to demonstrate multi-mode operation.

### 2.1. Orthosis Mechanical Design

The orthosis design consists of two parts: controller design and mechanical design. Mechanical design of the orthosis was performed using Solidworks. A simple design with two degrees of freedom (DoF) (*shoulder flexion/extension and elbow flexion/extension joints*) was used in the orthosis design to focus rehabilitation mode implementations, avoiding problems arising from complexity of mechanical design. The CAD drawing of the designed orthosis in Solidworks is given in Figure 1.

Physical parameters of the orthosis links, which were obtained from Solidworks, are given in Table 1; where  $I_i$  represents moment of inertia,  $m_i$  is the mass, and  $l_{ci}$  is the distance from the  $i$ -th joint to the  $i$ -th mass center position and  $l_i$  is the length of the  $i$ -th link.

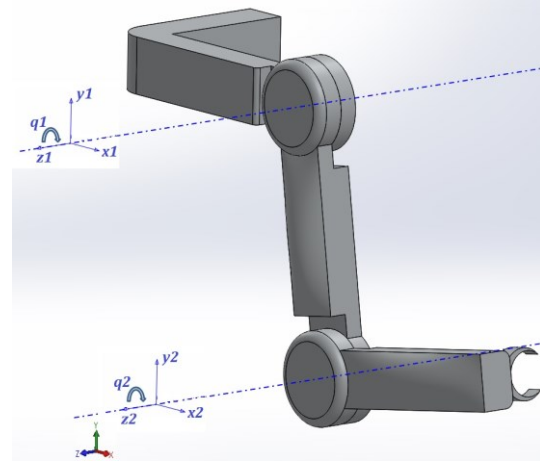


Figure 1. CAD drawing of the designed orthosis

Table 1. Physical parameters of the orthosis links

	$m_i$ [Kg]	$I_i$ [Kg m <sup>2</sup> ]	$l_{ci}$ [m]	$l_i$ [m]
$i=1$	1.72	0.05	0.13	0.28
$i=2$	1.74	0.04	0.12	0.27

Range of motions (ROM) of the orthosis joints has been restricted according to the values in the literature [16]. These ROM values are given in the Table 2.

Table 2. ROMs of the orthosis joints

Joint	ROM [Degree]
Shoulder Flexion	176
Shoulder Extension	66
Elbow Flexion	142
Elbow Extension	4

The orthosis dynamics were derived by using Lagrangian approach [17]. Dynamic model of the orthosis is in the standard form

$$M(q)\ddot{q}+V(q,\dot{q})\dot{q}+G(q)=\tau+\tau_h \quad (1)$$

with  $M(q)$  the inertia matrix,  $V(q,\dot{q})$  the Coriolis/Centripetal matrix,  $G(q)$  the gravity vector,  $q$  the vector of joint positions,  $\tau$  the joint actuator torques of the orthosis and  $\tau_h$  the arm

model's torque input . Details of  $M(q)$ ,  $V(q,\dot{q})$  and  $G(q)$  are given in Appendix A.

### 2.2. Human Arm Musculoskeletal Model

Musculoskeletal modelling of human arm was achieved with Musculoskeletal Modelling Software (MSMS). There are many software tools for musculoskeletal modelling such as SIMM (Software for Interactive Musculoskeletal Modelling) [18], OpenSim [19] and AnyBody (Anybody Technology, Aalborg, Denmark) [20]. However, the MSMS program was chosen in this work because it has General Public License (GPL) and permits conversion of musculoskeletal and orthosis models to Matlab/Simulink in order to perform simulation with controllers in place.

The muscle model used in MSMS is a modified Hill muscle model (Virtual muscle model) [15,21]. Hill muscle model estimates the muscle force as a function of muscle activation level, muscle parameters and joint kinematics [22]. It consists of active Contractile Element (CE), Parallel Element (PE) and Series Passive Element (SPE) [22–24] as shown in Figure 2. The CE refers to the contraction process that generates the active force. The SPE and PE components represent passive soft connective tissue including the tendon and the nonactive muscle fibers. Details of Hill muscle model are given in Appendix B.

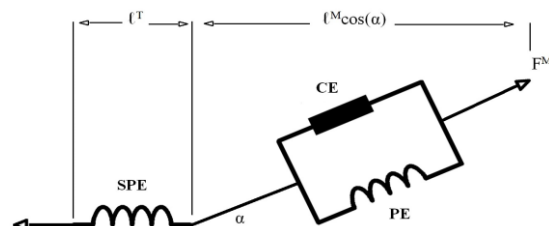


Figure 2. Schematic of the hill muscle model

MSMS version 2.2 was used in this work. This version contains some examples of human musculoskeletal models including the human upper limb. The muscles of this upper limb model have been modified, according to active joints and the muscle parameters in the literature and used in this paper. In the designed musculoskeletal model,

*Deltoid Anterior* and *Pectoralis Major Clavicular* muscles were used for shoulder flexion movement; *Deltoid Posterior* muscle was used for shoulder extension movement; *Biceps Long Head* and *Brachialis* muscles were used for elbow flexion movement; and *Triceps Long Head* and *Triceps Lateral Head* muscles were used for elbow extension movement. The muscle parameters which were obtained from studies in the literature [25–28] are given in Table 3.

Table 3. Muscle parameters used in MSMS

Muscle	Opt. Fascicle Length [cm]	Opt. Tendon Length [cm]	Max MT Length [cm]	Mass [g]
B. Long	15.6	19.11	37	80
Brachi.	8.6	5.67	15	338
Del. Ant.	10.1	2.73	16	410
Del. Post.	13.7	4	19	92
Pec. Maj.	14.4	0.315	19	214
T. Long	13.4	15.015	32	345
T. Lat.	11.4	10.29	24	273

The final state of the design obtained by transferring the CAD drawings of the orthosis to the MSMS environment is shown in Figure 3.

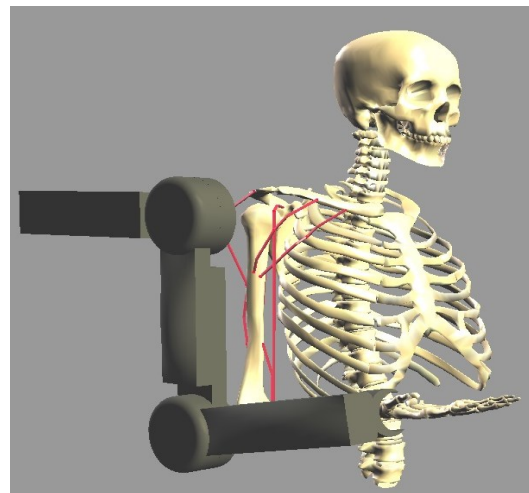
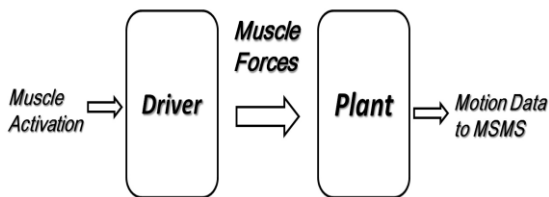


Figure 3. Orthosis and musculoskeletal model in MSMS platform

### 2.3. Orthosis and Musculoskeletal Model Implementation in Simulation

Simulation tool of MSMS, which converts musculoskeletal models to Simulink block diagrams, was used to transfer the designed orthosis and musculoskeletal model to Matlab/Simulink. The block diagram of the transferred model is given in Figure 4.



**Figure 4.** Block diagram of the transferred model from MSMS to Matlab/Simulink

The *Plant* Block shown in Figure 4 contains the mechanical models of the human skeleton and the orthosis. In the *Driver* Block, there are *S Function* blocks that contain the parameters of the muscles in the model and muscle path information.

The Virtual Muscle Model (*Musculoskeletal Model*) uses muscle activation as input. By using muscle activation information and muscle parameters, the forces generated by muscles are calculated. Muscle activation information is usually obtained by using EMG signals [29].

In this work, muscle activations were obtained by using PID controllers based on desired trajectories. Four PID controllers, one for the muscles responsible for the shoulder flexion motion (*Deltoid Anterior* and *Pectoralis Major Clavicular*), one for the muscle responsible for the shoulder extension motion (*Deltoid Posterior*), one for the muscles responsible for the elbow flexion motion (*Biceps Long Head* and *Brachialis*) and one for the muscles responsible for the elbow extension motion (*Triceps Long Head* and *Triceps Lateral Head*), were used. Differences between the joint positions of the musculoskeletal model and the trajectories of desired exercise tasks were used as PID controller inputs. Since the muscle activation could range from 0 to 1, the outputs of

the PID controllers were limited between these values by adding Simulink saturation blocks [23,29]. The schematic of the PID controller used for muscle activation is given in Figure 5.

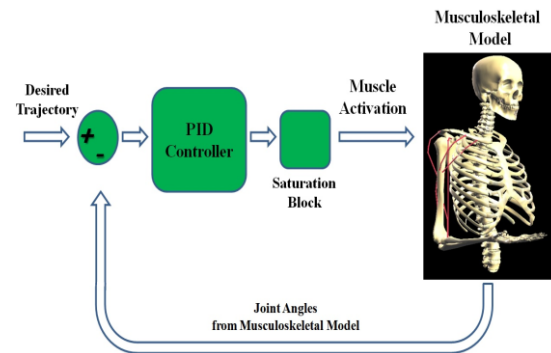


**Figure 5.** Schematic of the muscle activation PID controller

Orthosis is connected to human arm musculoskeletal model with body spring damper block in Simulink. This block is used to connect human arm model and orthosis in a flexible manner to simulate a real connection. It is also aimed to observe the interaction between arm model and orthosis during mode transitions. Human arm musculoskeletal model and orthosis have the same two active DoFs (*shoulder and elbow flexion/extension joints*) and they move on sagittal plane. Also, the orthosis link lengths were selected according to the musculoskeletal model links to avoid joint misalignments. Thus, it was ensured that the joint positions of the orthosis and musculoskeletal model were the same by using the body spring damper block. Body spring damper block's parameters were determined based on simulation studies.

### 2.4. Multi-Mode Model Based Controller

The main control approach for the orthosis was based on the computed torque control method. Computed torque controller is a model-based control method which uses the dynamic model of the system to compute the control torque signals that are input of the system [17]. This controller generally performs well when the robot arm dynamic parameters are known accurately and it

can also ensure globally asymptotic stability [30,31].

The designed controller consisted of two loops where inner loop was orthosis dynamics and outer loop was PID controller [32]. The PID computed torque controller method was chosen to avoid the complexity of intelligent control methods and to demonstrate that assistive and resistive rehabilitation modes could be realized with an easier-to-implement controller.

In the controller structure,  $u$  was the outer loop controlled variable,  $\tau$  was joint actuator torques,  $q$  and  $\dot{q}$  were joint position and velocity,  $q_d$ ,  $\dot{q}_d$  and  $\ddot{q}_d$  were desired joint position, velocity, and acceleration respectively. PID controller output signal was

$$u(t) = -(K_p e + K_v \dot{e} + K_i \int e(t) dt) \quad (2)$$

with  $e$  tracking error;  $e = (q_d - q)$ ,  $\dot{e} = \dot{q}_d - \dot{q}$  and  $\int e(t) dt$  the integral of the tracking error  $e(t)$ .  $K_p$ ,  $K_v$  and  $K_i$  are proportional, derivative and integral gains of the PID controller respectively. Those gain parameters were tuned by Ziegler Nichols method [33]. Detailed PID computed torque

controller block diagram is shown in Figure 6. For the Orthosis control, the following equation was used.

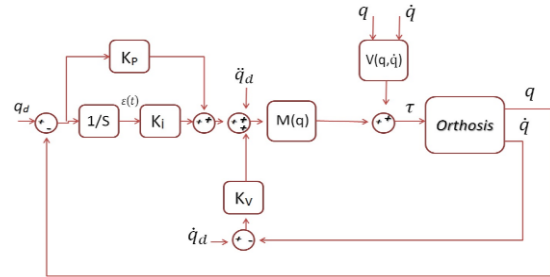


Figure 6. PID Computed Torque Controller block diagram

$$M(q) \left( \ddot{q}_d + K_p e + K_v \dot{e} + K_i \int e(t) dt \right) + V(q, \dot{q}) \dot{q} + G(q) = \tau + \tau_h \quad (3)$$

### 2.5. Assistive/Resistive Rehabilitation Modes and Mode Transitions

Controller assistive/resistive rehabilitation modes and transition between these modes was done by a Graphical User Interface (GUI) designed in Matlab. The designed GUI is shown in Figure 7.

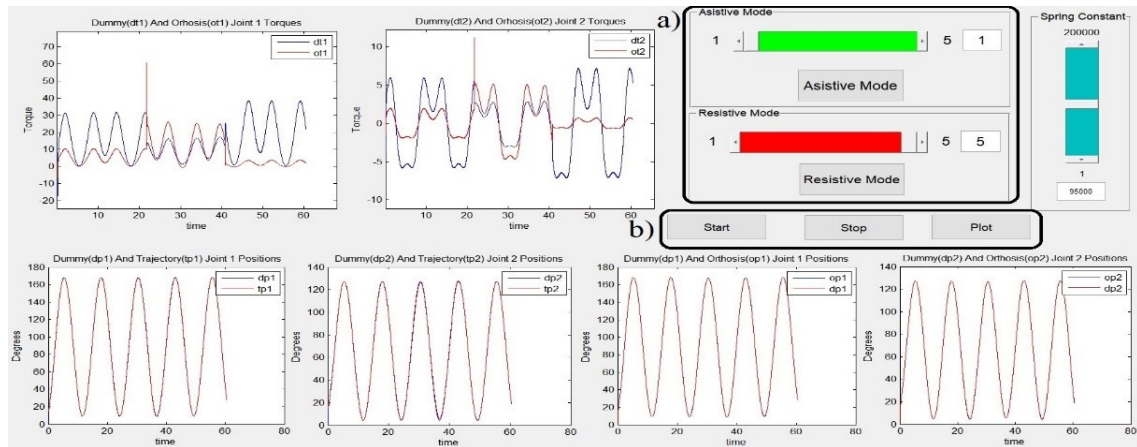
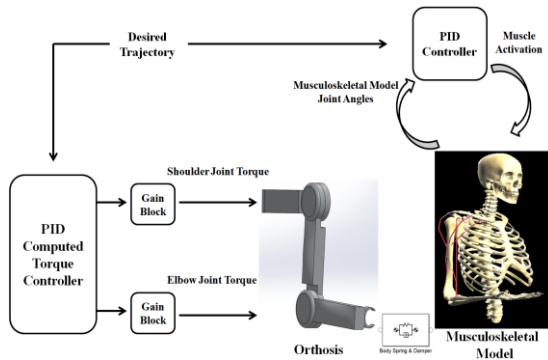


Figure 7. Matlab Graphical User Interface (GUI) a) Sections of assistive/resistive mode control panels, b) Start, stop and plot push buttons

Resistive and assistive modes of the orthosis were realized by gain adjustment blocks connected to torque outputs of the PID computed torque

controller ( $\tau$  in Equation 3), which was applied to orthosis joints as shown in Figure 8. By changing the gain values, in the assistive mode, joint

actuator torques of the orthosis ( $\tau$ ) were increased and in the resistive mode, these actuator torques ( $\tau$ ) were decreased.



**Figure 8.** Implementation of the assistive/resistive rehabilitation modes

Gain values were 1 at the beginning of the simulation which means the orthosis is at neither assistive nor resistive mode. This situation was stated as *normal mode* in results section. Gain values were adjusted larger than 1 when assistive mode was selected for proper operation. In this way, it was aimed to make the orthosis help movement of musculoskeletal model, and make the arm model complete its movement with less muscle force effort. The decrease in muscle forces demonstrates that the orthosis is assisting the movement of patient. In resistive mode, a challenging effect was created on movements of musculoskeletal model by choosing the gain values less than 1. With this effect, it was aimed to make patients spend more muscular force for

movements. This increase in muscle forces indicates that the patient is spending more efforts to complete the movement and thus, performing the rehabilitation exercises.

Assistive and resistive rehabilitation modes had 5 levels. Different levels of assistive and resistive modes were achieved by changing the gain values.

### 3. RESULTS AND DISCUSSIONS

The orthosis designed in this work were tested on a human arm musculoskeletal model. For desired exercise tasks, common trajectories were applied to the orthosis and musculoskeletal model joints as shown in Figure 8. The sinusoidal wave form was chosen as the desired trajectory to represent simple rhythmic movements used in rehabilitation exercises.

In the simulation, the orthosis was operated in normal mode (*Gain values equal to 1*) for first 40 seconds. Assistive mode was selected at a moment indicated by t1 marker. Orthosis has been switched to resistive mode at a moment indicated by t2 marker. t1 and t2 markers are shown in all relevant figures.

Musculoskeletal model and orthosis joint positions and desired trajectories for these joints are given in Figure 9.

The position errors of human arm musculoskeletal model joints are given in Figure 10.

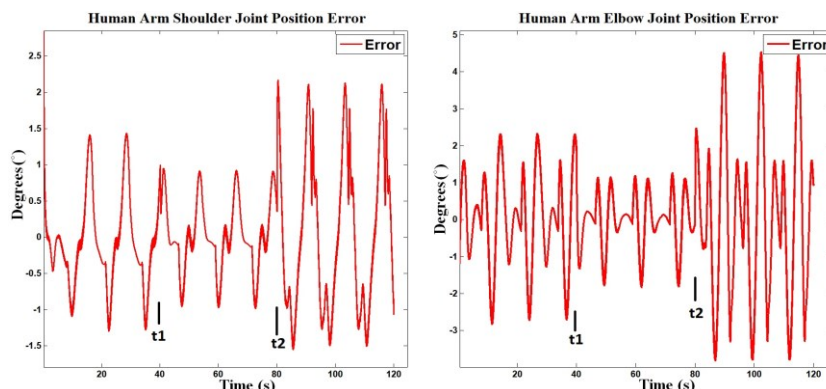


**Figure 9.** Human arm model and orthosis joint positions and desired trajectories

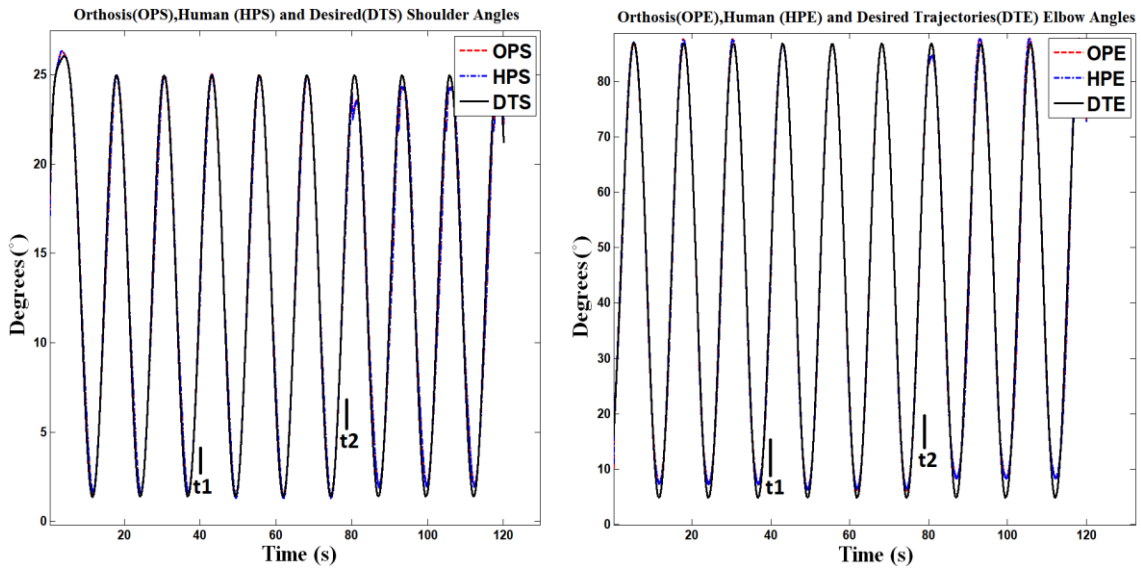


Figure 10. Human arm musculoskeletal model joint position errors

The decrease in joint position errors between moments of t1 and t2 shows that the orthosis supports trajectory tracking and performs assistive mode on the musculoskeletal model in coherence. The position errors were increased in both musculoskeletal model joints after the moment of t2. This increase in position errors is a result of the challenging effect that the orthosis applies to the

musculoskeletal model in resistive mode. Despite the increase in position errors, Figure 9 shows that the musculoskeletal model successfully follows the desired trajectory and completes the movement in the resistive mode. The orthosis joints actuators torques are given in Figure 11. The forces generated by the muscles of musculoskeletal model are given in Figure 12.

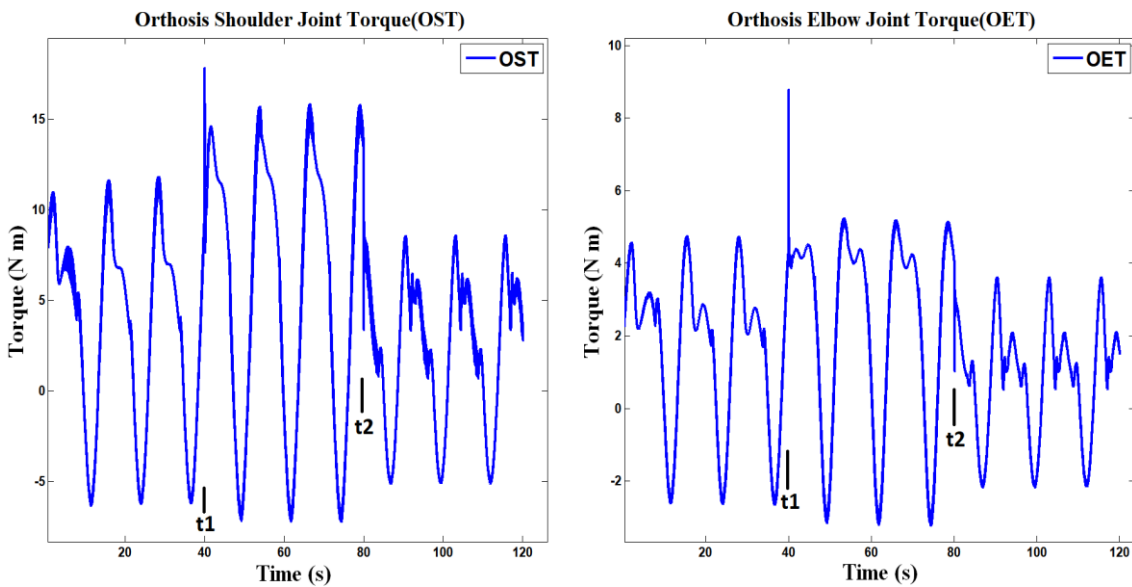


Figure 11. Orthosis joints actuator torques

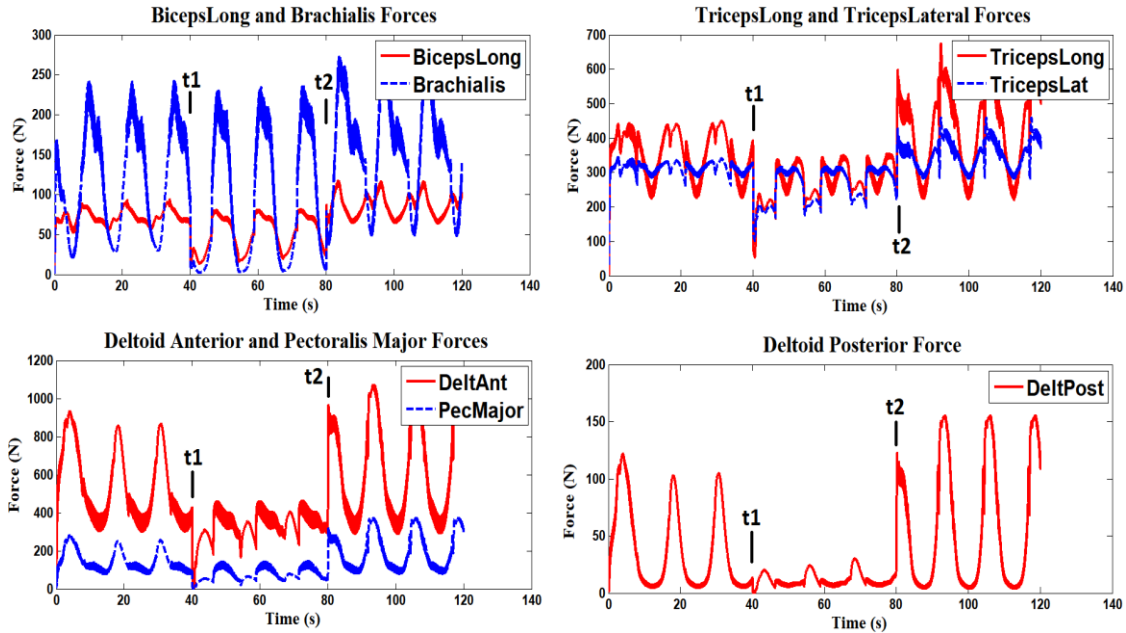


Figure 12. Muscle forces of the musculoskeletal model

Figure 11 shows, joint torques of orthosis increased for assisting to movement of the musculoskeletal model in the assistive mode, and in the resistive mode, joint torques decreased, compared to the normal mode, for making the arm model movement more difficult.

Figure 12 shows that Biceps Long force has decreased about 10 percent, Brachialis, Triceps Long, Triceps Lateral and Deltoid Posterior forces have decreased about 30 percent and Deltoid Anterior and Pectoralis Major forces have decreased about 50 percent after moment of  $t_1$  when the orthosis has gone into assistive mode. This decrease in muscle forces is a result of supporting the movement of the musculoskeletal model in the assistive mode by the orthosis. With this assistance, the musculoskeletal model could follow the desired trajectory with less muscle effort.

In the same figure, it is seen that after the moment of  $t_2$ , Biceps Long force has increased about 15 percent, Brachialis, Triceps Lateral, Deltoid Anterior and Pectoralis Major forces have increased about 30 percent and Triceps Long and

Pectoralis Major forces have increased about 50 percent when compared with the beginning. The increase in muscle forces indicates that the orthosis makes the movement of the musculoskeletal model more challenging and muscle forces increase to overcome this challenging effect in the resistive mode.

Simulation results demonstrate that the designed orthosis has applied assistive and resistive rehabilitation modes and mode transitions on the human arm musculoskeletal model successfully.

#### 4. CONCLUSIONS

In this work, a multi-mode, 2 DoF orthosis which enables assistive and resistive rehabilitation modes was designed. The designed orthosis has been tested in simulation on a musculoskeletal model created in the MSMS and Matlab/Simulink. In the musculoskeletal model, PID controllers were used to obtain muscle activation signals. PID computed torque controller was used in the orthosis control. The results obtained from the simulations show that the assistive and resistive rehabilitation modes of the designed orthosis and the mode transitions

have been successfully performed on the musculoskeletal model in coherence.

There are some orthotic devices for lower limb in the literature that perform assistive and resistive rehabilitation modes in combination [34]. However, there is no orthotic device available that performs these modes and mode transitions for the upper limb. In this work, assistive and resistive rehabilitation modes were successfully performed in a single device with known and easier-to-implement controllers such as PID and computed torque controller. It has also been shown by this work that the MSMS Program is a suitable and successful platform for the performance evaluation of orthotic devices.

Before directly going into a hardware implementation, an intelligent switching method for the mode transitions will be added to the controller structure in future works. Besides, with the addition of a high level controller to the controller structure, it is planned to reduce the joint position errors shown in Figure 10. Also, a detailed stability analysis is aimed to be performed before hardware implementation. Moreover, a hardware implementation is our eventual goal in the future.

## 5. APPENDIX

### 5.1. Dynamic Model of Orthosis

For  $i = 1, 2$ ,  $q_i$  denotes the joint angle,  $m_i$  denotes the mass of link  $i$ ,  $l_i$  and  $a_i$  denotes the length of link  $i$ ,  $l_{ci}$  denotes the distance from the previous joint to the center of mass of link  $i$ , and  $I_i$  denotes the moment of inertia of link  $i$  about an axis coming out of the page, passing through the center of mass of link  $i$ .

$$M(q) \begin{bmatrix} \ddot{q}_1 \\ \ddot{q}_2 \end{bmatrix} + \begin{bmatrix} -2m_2l_1l_{c2}\dot{q}_2\sin q_2 & -m_2l_1l_{c2}\dot{q}_2\sin q_2 \\ m_2l_1l_{c2}\dot{q}_1\sin q_2 & 0 \end{bmatrix} \begin{bmatrix} \dot{q}_1 \\ \dot{q}_2 \end{bmatrix}$$

$$+ \begin{bmatrix} (m_1l_{c1}+m_2l_1)g\sin q_1 + m_2l_{c2}g\sin(q_1+q_2) \\ m_2l_{c2}g\sin(q_1+q_2) \end{bmatrix} = \begin{bmatrix} \tau_1 \\ \tau_2 \end{bmatrix}$$

$$M(q) = \begin{bmatrix} m_1l_{c1}^2 + m_2l_1^2 + m_2l_{c2}^2 + 2m_2l_1l_{c2}\cos q_2 + I_1 + I_2 & \\ & m_2l_{c2}^2 + m_2l_1l_{c2}\cos q_2 + I_2 \end{bmatrix}$$

$$\begin{bmatrix} m_2l_{c2}^2 + m_2l_1l_{c2}\cos q_2 + I_2 \\ m_2l_{c2}^2 + I_2 \end{bmatrix}$$

### 5.2. Hill Muscle Model

The Zajac type Hill muscle model consists of 4 parameters, the optimum fascicle length ( $L_{CE0}$ ), the maximum isometric muscle force ( $F_{max}$ ), pennation angle ( $\alpha$ ) and the tendon slack length ( $L_S^T$ ) [23].

The forces generated by the Contractile Element and the Parallel Element are given in Equations below [23,29,35]. In these equations,  $a$  is muscle activation,  $f^l(\ell)$  represents force – length relationship of the muscle,  $f^v(v)$  represents force – velocity relationship of the muscle,  $f^{PE}$  is passive muscle force,  $\ell^M$  is muscle length,  $\ell^T$  is tendon length and  $\alpha$  is pennation angle. The force generated by Contractile Element is defined as

$$F_{ce} = f(\ell)f(v)aF_{(max)}$$

$$f(\ell) = \exp \left[ -0.5 \left( \frac{\frac{\Delta L_{CE} - 0.05}{L_{CE0}}}{0.19} \right)^2 \right]$$

$$f(v) = \frac{0.1433}{0.1074 + \exp(-1.3 \sinh(2.8(V_{CE}/V_{CE0}) + 1.64))}$$

$$V_{CE0} = 0.5(a+1)V_{CEmax}$$

$$V_{CEmax} = 10L_{CE0}$$

In these equations  $V_{CE0}$  is maximum CE contraction velocity when  $F_{ce} = 0$  and  $V_{CEmax}$  is  $V_{CE0}$  when muscle activation is maximum [35].

The force generated by Parallel Element is defined as

$$F_{PE} = \left[ \frac{F_{max}}{e^{S-1}} \right] \left[ e^{\left( \frac{S}{\Delta L_{max}} \Delta L \right)} - 1 \right]$$

where  $\Delta L$  is the change in length of the element with respect to the tendon slack length,  $S$  is a shape parameter (related to the stiffness of the element),

$F_{max}$  is the maximum force exerted by the element for the maximum change in length  $\Delta L_{max}$ .

Finally the total force developed by the muscle is equal to

$$F_{MT}=F_{CE}+F_{PE}$$

## 6. ACKNOWLEDGEMENT

This work is supported by Scientific Research Project Units of Çukurova University, in project FYL-2014-2541.

## 7. REFERENCES

- Volpe, B.T., Krebs, H.I., Hogan, N., 2001. Is Robot-aided Sensorimotor Training in Stroke Rehabilitation a Realistic Option? *Curr. Opin. Neurol.* 14, 745–752.
- Lum, P.S., Burgar, C.G., Shor, P.C., Majmundar, M., Van der Loos, M., 2002. Robot-assisted Movement Training Compared with Conventional Therapy Techniques for the Rehabilitation of Upper-limb Motor Function After Stroke. *Arch. Phys. Med. Rehabil.* 83, 952–959.
- Gopura, R.A.R.C., Kiguchi, K., 2009. Mechanical Designs of Active Upper-limb Exoskeleton Robots State-of-the-art and Design Difficulties. 2009 IEEE Int. Conf. Rehabil. Robot. ICORR 2009 178–187 doi:10.1109/ICORR.2009.5209630.
- Gopura, R.A.R.C., Bandara, D.S.V., Kiguchi, K., Mann, G.K.I. 2016. Developments in Hardware Systems of Active Upper-limb Exoskeleton Robots: A review. *Rob. Auton. Syst.* 75, 203–220
- Marchal-Crespo, L., Reinkensmeyer, D.J., 2009. Review of Control Strategies for Robotic Movement Training After Neurologic Injury. *J. Neuroeng. Rehabil.* 6, 20.
- Wolbrecht, E.T., Chan, V., Reinkensmeyer, D. J., Bobrow, J.E. 2008. Optimizing Compliant, Model-based Robotic Assistance to Promote Neurorehabilitation. *IEEE Trans. Neural Syst. Rehabil. Eng.* 16, 286–297.
- Lo, H.S., Xie, S.Q., 2012. Exoskeleton Robots for Upper-limb Rehabilitation: State of the Art and Future Prospects. *Med. Eng. Phys.* 34, 261–268.
- Anam, K., Al-Jumaily, A.A., 2012. Active Exoskeleton Control Systems: State of the Art. *Procedia Eng.* 41, 988–994.
- Lee, H.D., Lee, B.K., Kim, W.S., Han, J.S., Shin, K.S., Han, C.S., 2014. Human-robot Cooperation Control Based on a Dynamic Model of an Upper Limb Exoskeleton for Human Power Amplification. *Mechatronics* 24, 168–176.
- Rosen, J., Brand, M., Fuchs, M.B., Arcan, M., 2001. A Myosignal-based Powered Exoskeleton System. *IEEE Trans. Syst. Man, Cybern. Part A Systems Humans.* 31, 210–222.
- Sugar, T.G., He, J., Koeneman, E.J., Koeneman, J.B., Herman, R., Huang, H., Schultz, R.S., Herring, D.E., Wanberg, J., Balasubramanian, S., Swenson, P., Ward, J.A., 2007. Design and Control of RUPERT: A Device for Robotic Upper Extremity Repetitive Therapy. *IEEE Trans. Neural Syst. Rehabil. Eng.* 15, 336–346.
- Gopura, R.A.R.C., Kiguchi, K., Yi, Y., 2009. SUEFUL-7: A 7DOF Upper-limb Exoskeleton Robot with Muscle-model-oriented EMG-Based Control. 2009 IEEE/RSJ Int. Conf. Intell. Robot. Syst. IROS 2009 1126–1131, doi:10.1109/IROS.2009.5353935
- Crema, A., Mancuso, M., Frisoli, A., Selsedo F., Raschella, F., Micea, S., 2015. A Hybrid NMES-exoskeleton for Real Objects Interaction. *Int. IEEE/EMBS Conf. Neural Eng. NER 2015–July*, 663–666.
- Carignan, C., Tang, J., Roderick, S., 2009. Development of an Exoskeleton Haptic Interface for Virtual Task Training. 2009 IEEE/RSJ Int. Conf. Intell. Robot. Syst. IROS 2009 3697–3702, doi:10.1109/IROS.2009.5354834
- Davoodi, R., Loeb, G. E., 2011. MSMS Software for VR Simulations of Neural Prostheses and Patient Training and Rehabilitation. *Stud. Health Technol. Inform.* 163, 156–162.
- Moromizato, K., Kimura, R., Fukase, H., Yamaguchi, K., Ishida, H., 2016. Whole-body Patterns of the Range of Joint Motion in Young

- Adults: Masculine Type and Feminine Type. *J. Physiol. Anthropol.* 35, 23.
17. Lewis F.L., Munro N., 2004. *Robot Manipulator Control Theory and Practice*. Marcel Dekker, Inc.
  18. Delp, S. L., Loan, J. P., Hoy, M. G., Zajac, F. E., Topp, E.L., Rosen, J.M., 1990. An Interactive Graphics-based Model of the Lower Extremity to Study Orthopedic Surgical Procedures. *IEEE Trans. Biomed. Eng.* 37, 757–767.
  19. Delp, S.L., Anderson, F.C., Arnold, A.S., Loan, P., Habib, A., John, C.T., Guendelman, E., Thelen, D.G., 2007. OpenSim: Open Source to Create and Analyze Dynamic Simulations of Movement. *IEEE Trans. Biomed. Eng.* 54, 1940–1950.
  20. Damsgaard, M., Rasmussen, J., Christensen, S.T., Surma, E., de Zee, M., 2006. Analysis of Musculoskeletal Systems in the AnyBody Modeling System. *Simul. Model. Pract. Theory* 14, 1100–1111.
  21. Cheng, E.J., Brown, I.E., Loeb, G.E., 2001. Virtual Muscle: A Computational Approach to Understanding the Effects of Muscle Properties on Motor Control. *J. Neurosci. Methods* 106, 111–112.
  22. Rosen, J., Fuchs, M. B., Arcan, M., 1999. Performances of Hill-Type and Neural Network Muscle Models-Toward a Myosignal-Based Exoskeleton. *Comput. Biomed. Res.* 32, 415–439.
  23. Zajac, F.E., 1989. Muscle and Tendon: Properties, Models, Scaling, and Application to Biomechanics and Motor Control. *Crit. Rev. Biomed. Eng.* 17, 359–411.
  24. Winters, J. M., 1995. An Improved Muscle-Reflex Actuator for use in Large-scale Neuromusculoskeletal Models. *Ann. Biomed. Eng.* 23, 359–374.
  25. Garner, B.A., Pandy, M.G., 2001. Musculoskeletal Model of the Upper Limb Based on the Visible Human Male Dataset. *Comput. Methods Biomech. Biomed. Engin.* 4, 93–126.
  26. Langenderfer, J., Jerabek, S.A., Thangamani, V.B., Kuhn, J.E., Hughes, R.E., 2004. Musculoskeletal Parameters of Muscles Crossing the Shoulder and Elbow and the Effect of Sarcomere Length Sample Size on Estimation of Optimal Muscle Length. *Clin. Biomech.* 19, 664–670.
  27. Holzbaur, K.R.S., Murray, W.M., Delp, S.L., 2005. A Model of the Upper Extremity for Simulating Musculoskeletal Surgery and Analyzing Neuromuscular Control. *Ann. Biomed. Eng.* 33, 829–840.
  28. Saul, K.R., Hu X., Goehler C.M., Vidt M.E., Daly M., Velisar A., Murray W.M., 2014. Benchmarking of Dynamic Simulation Predictions in Two Software Platforms using an Upper Limb Musculoskeletal Model. *Comput. Methods Biomech. Biomed. Engin.* 18, 1–14.
  29. Buchanan, T.S., Lloyd, D.G., Manal, K., Besier, T.F., 2004. Neuromusculoskeletal Modeling: Estimation of Muscle Forces and Joint Moments and Movements from Measurements of Neural Command. *J. Appl. Biomech.* 20, 367–95.
  30. Song, Z., Yi, J., Zhao, D., Li, X., 2005. A Computed Torque Controller for Uncertain Robotic Manipulator Systems: Fuzzy Approach. *Fuzzy Sets Syst.* 154, 208–226.
  31. Han, S., Wang, H., Tian, Y., 2017. Integral Backstepping Based Computed Torque Control for a 6 DOF Arm Robot. *Proc. 29<sup>th</sup> Chinese Control Decis. Conf. CCDC 2017* 4055–4060. doi:10.1109/CCDC.2017.7979210
  32. Craig J.J., 2005. *Introduction to Robotics*. Pearson Education Inc., doi:10.1111/j.1464-410X.2011.10513.x
  33. Ogata K., 2009. *Modern Control Engineering*. Pearson Prentice Hall.
  34. Chandrapal, M., Chen, X., 2009. Intelligent Active Assistive and Resistive Orthotic Device for Knee Rehabilitation. *2009 IEEE Int. Conf. Control Autom. ICCA 2009* 1880–1885 doi:10.1109/ICCA.2009.5410528
  35. Cavallaro, E., Rosen, J., Perry, J.C., Burns, S., Hannaford, B., 2005. Hill-based Model as a Myoprocessor for a Neural Controlled Powered Exoskeleton Arm-Parameters Optimization. *Proc. - IEEE Int. Conf. Robot. Autom.* 2005, 4514–4519.